

Superparamagnetic core-shell polymer particles for efficient purification of his-tagged proteins†

WeiJun Fang, Xiaolan Chen and Nanfeng Zheng*

Received 1st July 2010, Accepted 12th August 2010

DOI: 10.1039/c0jm02081h

Magnetic core-shell $\text{Fe}_3\text{O}_4@\text{SiO}_2@\text{poly}(\text{styrene-alt-maleic anhydride})$ spheres enriched with Ni-NTA on their surface have been prepared by precipitation polymerization. The spheres have a core composed of superparamagnetic polycrystalline magnetite having a uniform size of ~ 220 nm, endowing the spheres with excellent magnetic responsivity and dispersity. The shell composition of poly(styrene-alt-maleic anhydride) allows the incorporation of more Ni-NTA affinity sites onto the surface of the magnetic spheres. Owing to the multivalency effect, the separation capacity of His-tagged proteins by the as-prepared $\text{Fe}_3\text{O}_4@\text{SiO}_2@\text{polymer}/\text{Ni-NTA}$ composites was four times as that by $\text{Fe}_3\text{O}_4@\text{SiO}_2/\text{Ni-NTA}$, making them particularly promising for the magnetic separation of low-concentration His-tagged proteins. The magnetic polymer hybrid particles also exhibited excellent performance in the direct separation of His-tagged proteins from cells lysates.

Introduction

The development of fast and efficient methods to separate proteins of interest from a biological source remains a challenging task in the proteomic era. Currently, placing affinity tags at desired position of the proteins has been widely used to facilitate the protein separation. One of the most popular tags is polyhistidine which binds strongly to divalent metal ions such as Ni^{2+} and Co^{2+} . Nickel ion affinity chromatography has therefore become the most commonly method to separate His-tagged proteins.¹ To isolate the targeted His-tagged proteins from crude cell lysates using the ion affinity chromatography method, it is often necessary to remove cellular debris and time-consuming. Therefore, alternative purification methods that allow the direct and rapid separation of His-tagged proteins from cell lysates are highly demanded. Fortunately, magnetic separation using magnetic nanoparticles binding with affinity agents has recently been demonstrated as one of such effective methods.

In the past decade, magnetic nanoparticles have been extensively studied for various biological applications,² such as magnetic resonance imaging (MRI),^{3–5} drug delivery,^{6–8} magnetofection,⁹ hyperthermia treatment of cancer, and bioseparation.^{10–12} With the use of magnetic nanoparticles, the separation of cells, DNA and proteins can be significantly simplified by applying an external magnetic field.^{13–16} To magnetically separate His-tagged proteins from cell lysates, the key is to couple the appropriate affinity agents on the surface of magnetic nanoparticles. For instance, Xu and co-workers modified FePt and

Co/Fe₂O₃ magnetic nanoparticles with nickel nitrilotriacetic acid (Ni-NTA) to separate His-tagged proteins.^{17,18} By modifying superparamagnetic iron oxide nanoparticles with multivalent Ni-NTA, Lin and co-workers demonstrated their enhanced capability in separating His-tagged proteins at low concentration.¹⁹ The drawback of these studies was that the diameter of the magnetic nanoparticles was ~ 10 nm, leading to the difficult separation of particles from solutions. In addition of Ni-NTA, NiO was also reported having good affinity with polyhistidine tagged proteins.²⁰ Hyeon and co-workers have successfully prepared Ni/NiO core/shell nanoparticles for magnetic separation of His-tagged proteins.²¹ However, these nanoparticles were prone to be oxidized by air and thus magnetically unstable. To tackle the stability issue, Lee's group prepared core/shell iron oxide@NiO nanoparticles for the separation.²² However, the nanoparticles had a diameter of ~ 10 nm and relatively weak magnetic characteristics. Very recently, Hyeon and co-workers decorated the core-shell magnetic $\text{Fe}_3\text{O}_4@\text{SiO}_2$ microspheres with NiO nanoparticles and demonstrated their excellent recyclability in the separation His-tagged proteins.²³

Compared to Ni-NTA, the non-specific binding of non-tagged proteins on NiO is less documented. To improve the magnetic separation efficiency of His-tagged proteins and suppress the non-specific binding of non-tagged proteins, we have now developed a facile route to prepare magnetic core-shell $\text{Fe}_3\text{O}_4@\text{SiO}_2@\text{poly}(\text{styrene-alt-maleic anhydride})$ ($\text{Fe}_3\text{O}_4@\text{SiO}_2@\text{P}(\text{St-alt-MAN})$) microspheres enriched with Ni-NTA on their surface. The core is composed of superparamagnetic polycrystalline magnetite having a size of ~ 220 nm, which endows the core-shell spheres with excellent magnetic responsivity and dispersity. The shell composition of poly(styrene-alt-maleic anhydride)P(St-alt-MAN) allows the incorporation of more Ni-NTA affinity sites onto the surface of the magnetic spheres. As compared to $\text{Fe}_3\text{O}_4@\text{SiO}_2/\text{Ni-NTA}$ with the direct coupling of Ni-NTA on silica, the as-prepared $\text{Fe}_3\text{O}_4@\text{SiO}_2@\text{polymer}/\text{Ni-NTA}$ composites significantly enhance the magnetic separation performance of His-tagged proteins in low concentration.

State Key Laboratory for Physical Chemistry of Solid Surfaces and Department of Chemistry Xiamen University, College of Chemistry and Chemical Engineering, Xiamen, 361005, China. E-mail: nfheng@xmu.edu.cn; Tel: +86 -592- 2186821

† Electronic supplementary information (ESI) available: Zeta potentials of different intermediate particles, TGA curves of $\text{Fe}_3\text{O}_4 @\text{SiO}_2/\text{polymers}$, the hysteresis loops of the magnetic particles and fluorescence spectra of GFP solutions with the addition of magnetic particles. See DOI: 10.1039/c0jm02081h

Experimental section

Materials

Styrene(St) was washed two times by 10% NaOH solution, dried by calcium chloride and distilled under reduced pressure before use. Azo-bis-isobutyronitrile (AIBN) was recrystallized twice from absolute ethanol. Maleic anhydride(MAn) was used as received. Methacrylic acid was dried over 4 Å molecular sieves and distilled under reduced pressure. Toluene was dried over calcium chloride. p-Divinyl benzene (DVB) and all other reagents were used as received without further purification.

Preparation of Fe₃O₄ nanoparticles

The Fe₃O₄ spheres were prepared by the solvothermal reaction. 270 mg of FeCl₃ · 6H₂O, and 328 mg of NaOAc were dissolved in 8 mL of ethylene glycol, followed by the addition of 8 mL of poly ethylene glycol (600) under stirring. The obtained homogeneous yellow solution was sealed in Teflon-lined stainless-steel autoclaves, heated from 30 °C to 180 °C for 2 h, and maintained at 180 °C for 12 h. The obtained Fe₃O₄ spheres were washed by ethanol and water for several times, and finally re-dispersed in ethanol (8 mL) for further use.

Preparation of Fe₃O₄@SiO₂ core-shell particles

The Fe₃O₄@SiO₂ Core-shell spheres were prepared according to the Stöber method. 40 mg of Fe₃O₄, 6 mL of concentrated ammonia and 80 mL of water were mixed with 320 mL of ethanol. After ultrasonication for 10 min, 0.22 mL of tetraethoxysilane(TEOS) was added to the mixture with continuous stirring. After the reaction for more than 8 h, the obtained product was collected by a magnet, washed by water and absolute ethanol, and re-dispersed in 4 mL of ethanol for further use.

Preparation of Fe₃O₄@SiO₂-NH₂ core-shell particles

40 mg of Fe₃O₄@SiO₂ core-shell particles, 40 mL of ethanol, and 0.04 mL of 3-aminopropyltrimethoxysilane (APS) were mixed and refluxed overnight. The Fe₃O₄@SiO₂-NH₂ particles were separated with a magnet and washed with ethanol and DMF, and finally re-dispersed in 4 mL of DMF for subsequent use.

Preparation of Fe₃O₄@SiO₂/NTA particles

2.0 mg of Fe₃O₄@SiO₂-NH₂ particles were dispersed in the PBS solution (1.5 ml) with ultrasonication. Thereafter, 25% glutaraldehyde (GLH) solution was added and the reaction was aged for 8 h at room temperature. The magnetic particles were washed with PBS for three times and dispersed in the PBS solution (1.0 mL), followed by the addition of 1.2 mg of nitrilotriacetic acid (NTA). After more than 8 h, 0.5 mg of NaBH₄ was added to the above solution. After stirred for 2 h, the products were separated, washed with PBS, and re-dispersed in PBS for subsequent use.

Preparation of Fe₃O₄@SiO₂/P(St-alt-MAA)/NTA particles

5.0 mg of Fe₃O₄@SiO₂-NH₂ particles, 50 µL of methacrylic acid and 0.1 g of dicyclohexylcarbodiimide (DCC) were mixed in 5.0 mL of dry DMF. After stirred for 8 h at 40 °C, the particles

were separated, washed with DMF and dispersed in 10 mL of toluene. The obtained dispersion was then transferred into a three-necked flask together with MAn (0.15g, 1.5 mmol), St (0.16 mL, 1.4 mmol) and p-divinyl benzene (DVB) (7.5 µL). After degassing with nitrogen for 10 min, the solution was heated up to 75 °C. 0.5 mL AIBN solution (20 mg/mL) was injected to the mixture. After reaction for 1.5 h, the magnetite/polymer core/shell structure were obtained, and washed with dry DMF for five times to remove the physioadsorbed polymer, and then redispersed in 1.0 mL of PBS solution containing of NTA (1.2 mg) and triethylamine (5.0 µL). After 8 h of reaction, the final particles were separated, washed with PBS, and re-dispersed in PBS for subsequent use.

Preparation of Fe₃O₄@SiO₂/Ni-NTA and Fe₃O₄@SiO₂/P(St-alt-MAA)/Ni-NTA Particle

Fe₃O₄@SiO₂/NTA or Fe₃O₄@SiO₂@poly(styrene-alt-maleic acid)/NTA (Fe₃O₄@SiO₂/P(St-alt-MAA)/NTA) solution was added 1.0 mL Ni(CH₃COO)₂ solution (0.1 M) and shaken for 1 h. Then, the product was separated from the solution and washed two times with PBS.

Activity of the nanoparticles for separation of His-tagged proteins

20 µg of Fe₃O₄@SiO₂/Ni-NTA or Fe₃O₄@SiO₂/P(St-alt-MAA)/Ni-NTA particles were added to 6.0µg of His-tagged GFP or OFP without his-tag solution (PBS buffer, 10µL) and incubated for 10 min on the ice. The particles were separated by a magnet, and incubated with imidazole solution (3 M, 25µL) for 10 min to release the captured proteins.

Recyclability of magnetic spheres for separation of His-tagged proteins

Magnetic spheres used were collected for recycling experiment. In a typical procedure, 20 µg of Fe₃O₄@SiO₂/Ni-NTA or 12 µg of Fe₃O₄@SiO₂/P(St-alt-MAA)/Ni-NTA particles were washed with 10 µL PBS two times, then incubated with 50 mM EDTA in PBS buffer for 20 min, mixed with Ni(CH₃COO)₂ solution (0.1 M, 20 µL). After washed with 10 µL PBS, the magnetic spheres were incubated with His-tagged GFP solution to investigate their separation performance.

Capability of magnetic spheres for separation of His-tagged proteins

6.0 µg of His-tagged protein was mixed with different amount of Fe₃O₄@SiO₂/Ni-NTA or Fe₃O₄@SiO₂/P(St-alt-MAA)/Ni-NTA particles. 10 µg, 20 µg, 30 µg, 40 µg, 48 µg of Fe₃O₄@SiO₂/Ni-NTA particles were incubated with 6.0 µg of His-tagged GFP in PBS on the ice. After separation magnetic spheres, the reactive solution was added to 1.0 mL PBS and detected the fluorescent intensity of the solution. The same experimental produce carried out with variation on the amount of Fe₃O₄@SiO₂/P(St-alt-MAA)/Ni-NTA particles from 5 µg to 12 µg.

Binding affinity of magnetic spheres to His-tagged proteins

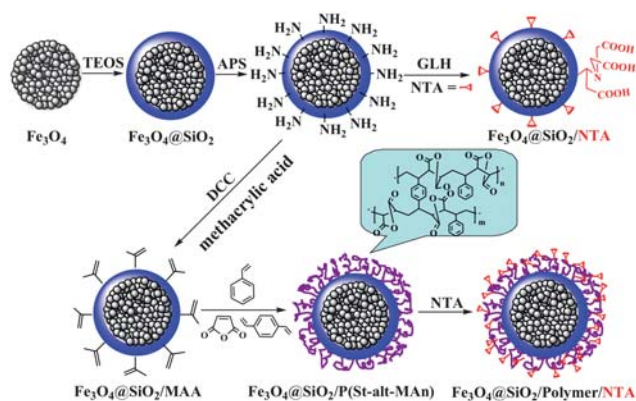
6.0 μg of His-tagged proteins were incubated with 20 μg of Ni(II)-loaded particles in different concentration. Briefly, 20 μg of $\text{Fe}_3\text{O}_4@\text{SiO}_2/\text{Ni-NTA}$ particles were incubated with 6.0 μg of His-tagged GFP in 5 μL , 50 μL or 500 μL PBS buffer on the ice. After separation magnetic spheres, the reactive solution was added to 995 μL , 950 μL or 500 μL of PBS buffer for detecting the fluorescent intensity of the solution. The same experimental procedure was carried out with $\text{Fe}_3\text{O}_4@\text{SiO}_2/\text{Ni-NTA}$ particles.

Expression and purification of His-tagged proteins in *E. coli*

The gene for expression of GFP or human p16 was cloned in PET-32a vector, and transformed into *E. coli* BL21(DE3) cells. The BL21(DE3) cells was grown in LB medium (10 g/L tryptone, 5 g/L yeast extract, and 10 g/L NaCl) until OD600 reached 0.8, 0.4 mM IPTG (isopropyl-1-thio- β -D-galactopyranoside) added to the culture and induced for 6 h at 30 $^\circ\text{C}$. The bacterial cells were collected by centrifugation with 6000 rpm at 4 $^\circ\text{C}$, re-dispersed in 1.0 mL PBS (phosphate-buffered saline) with 1.0 mM PMSF. After disrupting the cell by sonication on the ice with 12 s, the cell lysate was separated from cellular debris by centrifugation at 10,000 rpm for 20 min. The supernatant was incubated with the magnetic particles in an ice bath for 10 min. Using a magnet, the particles were collected, and washed with a PBS solution containing imidazole. SDS-PAGE (sodium dodecylsulfate – polyacrylamide gel electrophoresis) was used for the analysis the washed proteins. The SDS-PAGE gel was stained with Coomassie Blue more than 2 h.

Results and discussion

Scheme 1 illustrates the detailed procedure for creating superparamagnetic core-shell particles containing a polymeric shell (see the Experimental Section for details) for the separation of His-tagged proteins. In brief, the superparamagnetic Fe_3O_4 nanospheres were first prepared using the modified method reported by Li *et al.*²⁴ Due to the easy aggregation of Fe_3O_4 nanospheres, the synthesis of monodispersed Fe_3O_4 nanospheres in our systems was optimized by adding an appropriate amount of polyethylene glycol and also reducing the amount of sodium acetate. As shown in Fig. 1b, the as-produced Fe_3O_4 nanospheres



Scheme 1 Synthetic procedure for the magnetite/polymer core/shell structure spheres. GLH = glutaraldehyde.

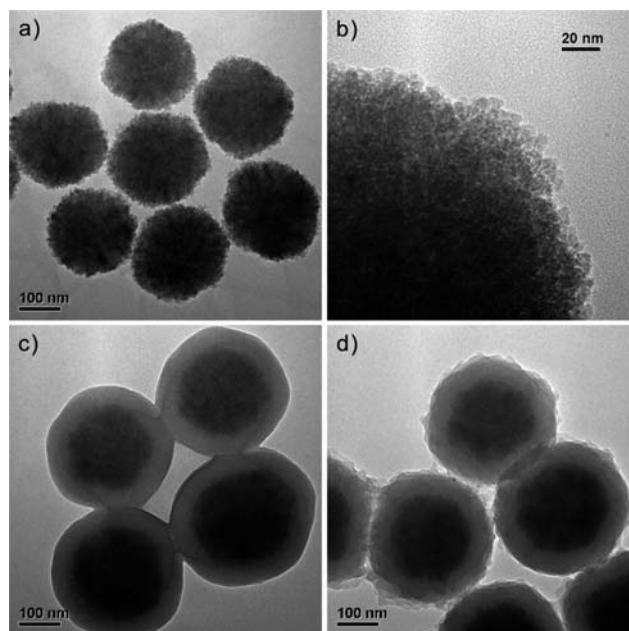


Fig. 1 TEM images of a) and b): Fe_3O_4 particles c): $\text{Fe}_3\text{O}_4@\text{SiO}_2$ spheres and d): $\text{Fe}_3\text{O}_4@\text{SiO}_2/\text{P}(\text{St-alt-MAN})$ spheres.

were composed of many fine primary magnetite nanocrystals having an average size of 4 nm. The overall size of the Fe_3O_4 nanospheres was 220 nm. The XRD pattern of the as-prepared Fe_3O_4 spheres matches that of inverse spinel magnetite (Fe_3O_4) (JCPDS 82-1533) (Fig. S1). The Fe_3O_4 spheres were then coated with a layer of silica through the Stöber method. The silica coating had a thickness of ~ 50 nm. While the surface of Fe_3O_4 spheres was rather rough, the surface of the particles became smooth after being coated with silica (Fig. 1,2). The layer of silica would protect the magnetic spheres from oxidation and also serve as a convenient platform for the surface functionalization of the superparamagnetic nanospheres. In this study, the surface of silica was modified with Ni-NTA groups which have been widely demonstrated as effective motifs to separate His-tagged proteins. Such a surface modification was achieved in two approaches. In one approach, Ni-NTA groups were directly anchored to the silica surface through organic silica. In the other approach, the $\text{Fe}_3\text{O}_4@\text{SiO}_2$ core-shell nanospheres were coated with a layer of organic polymer bearing abundant anhydride groups through which Ni-NTA groups were coupled onto the surface of the magnetic particles. Compared to the direct coupling of Ni-NTA on silica, an obvious advantage of the

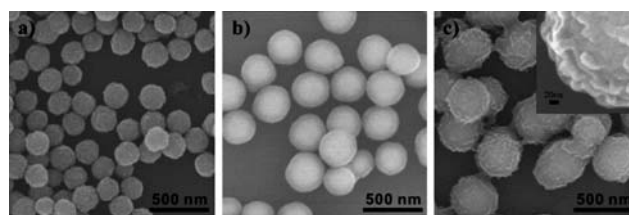


Fig. 2 SEM images of a) Fe_3O_4 particles b) $\text{Fe}_3\text{O}_4@\text{SiO}_2$ spheres and c) $\text{Fe}_3\text{O}_4@\text{SiO}_2/\text{P}(\text{St-alt-MAN})$. The inset is the corresponding SEM image with higher magnification.

polymer-mediated coupling of Ni-NTA groups is that more Ni-NTA sites can be incorporated onto each Fe_3O_4 nanosphere, which helps to improve the efficiency of the magnetic separation.

To directly couple Ni-NTA groups, the surface of $\text{Fe}_3\text{O}_4@/\text{SiO}_2$ was first silanized with 3-aminopropyltriethoxysilane (APS) by refluxing in ethanol to form the $\text{Fe}_3\text{O}_4@/\text{SiO}_2\text{-NH}_2$ spheres. Glutaraldehyde, having two aldehyde groups, was then applied to link 6-Amino-2-(bis-carboxymethyl-amino)-hexanoic acid onto the surface of $\text{Fe}_3\text{O}_4@/\text{SiO}_2\text{-NH}_2$.²⁵ In order to demonstrate the successful anchoring of NTA motifs on the spheres, the zeta potential of the nanospheres after each surface modification step was measured. As shown in Fig. S2, the modification of amino groups on the surface of $\text{Fe}_3\text{O}_4@/\text{SiO}_2$ changed their zeta potential from -23.7 mV to $+27.0$ mV in ultra-pure water. After NTA groups were linked on the surface by the glutaraldehyde linkers, the average zeta potential went back to -15.5 mV due to the presence of carboxyl groups on the surface of the magnetic spheres.

In order to achieve more Ni-NTA binding sites on each $\text{Fe}_3\text{O}_4@/\text{SiO}_2$, a layer of polymer was coated on their surface and used as a mediator. The silica surface of the spheres was first modified with C=C double bonds by coupling methacrylic acid molecules onto the surface of $\text{Fe}_3\text{O}_4@/\text{SiO}_2\text{-NH}_2$ using dicyclohexylcarbodiimide (DCC) as a coupling reagent. The vinyl groups on the surface of the resulted $\text{Fe}_3\text{O}_4@/\text{SiO}_2/\text{MA}$ spheres were then utilized to produce thereon a layer of cross-linked polymer bearing carboxylic groups. The precipitation polymerization on the magnetic spheres was carried out by using styrene and maleic anhydride as the monomers, and divinylbenzene as the cross-linkers in the presence of 2,2'-azobisisobutyronitrile (AIBN) as the initiator. After polymerization, a rugged layer of polymer was clearly observed in both TEM and SEM images (Fig. 1, 2), indicating the successful growth of poly(styrene-alt-maleic anhydride) (P(St-alt-MAN)) on the surface of the magnetic spheres. The polymer continuously wrapped around the surface with the formation of some particulates thereon.

Infrared spectroscopy (IR) was also used to confirm the polymer formation. As revealed in Fig. 3, $\text{Fe}_3\text{O}_4@/\text{SiO}_2\text{-NH}_2$ spheres have two characteristic peaks at ~ 1092 cm^{-1} and 590 cm^{-1} ,²⁶

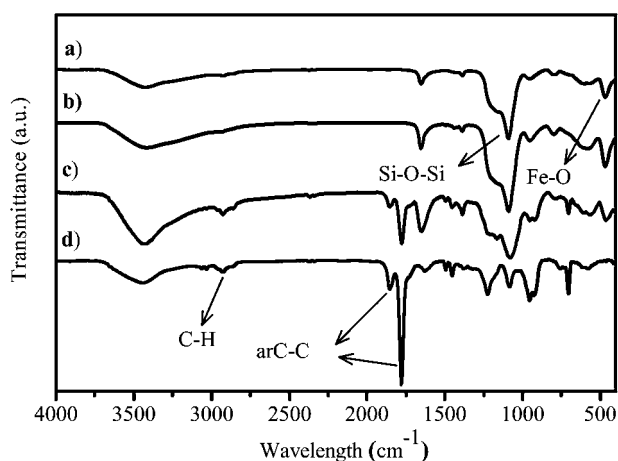


Fig. 3 IR spectra of a) $\text{Fe}_3\text{O}_4@/\text{SiO}_2\text{-NH}_2$ spheres, b) $\text{Fe}_3\text{O}_4@/\text{SiO}_2/\text{MA}$ spheres, c) $\text{Fe}_3\text{O}_4@/\text{SiO}_2/\text{P(St-alt-MAN)}$ spheres, and d) Poly(Stryene-alt-maleic anhydride).

corresponding to the vibration of Si-O-Si and Fe-O bonds, respectively. After coated with P(St-alt-MAN), three additional strong absorption peaks appeared. While the peak at 2930 cm^{-1} is attributed to the stretching of C-H bond, the two peaks at 1780 and 1855 cm^{-1} arise from the C-C bond vibration of benzene rings.²⁷ Similar IR spectrum was also observed on the bare P(St-alt-MAN) prepared under the same condition but in the absence of the inorganic $\text{Fe}_3\text{O}_4@/\text{SiO}_2$ core.

Thermogravimetric analysis (TGA) curves for magnetic spheres are shown in Fig. S3. When heated up to 800 $^{\circ}\text{C}$, $\text{Fe}_3\text{O}_4@/\text{SiO}_2/\text{MA}$ spheres had a total weight loss of $\sim 13\%$ with a major weight loss occurring between 160 and 320 $^{\circ}\text{C}$, which is probably corresponding to the release of high boiling point solvent absorbed on the surface and the decomposition of methacrylic acid molecules. In comparison, $\text{Fe}_3\text{O}_4@/\text{SiO}_2/\text{P(St-alt-MAN)}$ spheres had two obvious weight loss stages when heated in air up to 800 $^{\circ}\text{C}$. The total weight loss was about 34% , indicating that a significant amount of P(St-alt-MAN) were successful coated onto the magnetic spheres. While the weight loss between 280 and 350 $^{\circ}\text{C}$ might be due to the decomposition of anhydride groups of P(St-alt-MAN), the loss between 400 and 500 $^{\circ}\text{C}$ is likely attributed to the burning of the polymer's bone.

The successful coating of P(St-alt-MAN) layer is important to increase the Ni-NTA loading on the magnetic spheres because the polymer provides abundant reactive anhydride groups and therefore carboxylic groups after being hydrolyzed for further chemical or biological modification. Here we made use of the amino groups on the NTA molecules to react with the anhydride groups on the P(St-alt-MAN) layer to introduce the NTA motifs on the surface of the magnetic particles. The nanospheres were then dispersed in a Ni(II) solution to create the Ni-NTA groups for the separation of His-tagged proteins. Inductively coupled plasma mass spectrometry (ICP-MS) was used to quantify the amount of nickel ions on the surface of the magnetic spheres. As revealed by the measurements, the loading of Ni(II) in the as-made $\text{Fe}_3\text{O}_4@/\text{SiO}_2/\text{P(St-alt-MAN)}/\text{Ni-NTA}$ spheres was 87 $\mu\text{g}/\text{mg}$ which is three times as that in the $\text{Fe}_3\text{O}_4@/\text{SiO}_2/\text{Ni-NTA}$ spheres (29 $\mu\text{g}/\text{mg}$). The increased loading of Ni(II) in the $\text{Fe}_3\text{O}_4@/\text{SiO}_2/\text{P(St-alt-MAN)}/\text{NTA}$ is due to the more NTA molecules linked to the surface. Finally, we used superconducting quantum interference device (SQUID) for characterize the magnetic behavior of these magnetic spheres (Fig. S4). The result shows that the superparamagnetic core-shell hybrid particles have strong magnetization, suggesting its suitability for magnetic separation. As compared to 75 emu g^{-1} for the bare Fe_3O_4 spheres, the magnetization of the magnetic polymer hybrid particles were reduced to 30 emu g^{-1} , which is attributed due to the additional weight of the SiO_2 and polymer coating.

To demonstrate the efficiency of both $\text{Fe}_3\text{O}_4@/\text{SiO}_2/\text{Ni-NTA}$ and $\text{Fe}_3\text{O}_4@/\text{SiO}_2/\text{P(St-alt-MAN)}/\text{Ni-NTA}$ in magnetically separating His-tagged proteins, green fluorescent protein (GFP) was used as a model protein. Briefly, a required amount of $\text{Fe}_3\text{O}_4@/\text{SiO}_2/\text{Ni-NTA}$ or $\text{Fe}_3\text{O}_4@/\text{SiO}_2/\text{P(St-alt-MAN)}/\text{Ni-NTA}$ particles were incubated with GFP on the ice for 10 min. After using a magnet to collect the magnetic particles, the remnant GFP in the solution was measured by the spectrofluorophotometer. As illustrated in Fig. 4a, after incubated with $\text{Fe}_3\text{O}_4@/\text{SiO}_2/\text{Ni-NTA}$ and $\text{Fe}_3\text{O}_4@/\text{SiO}_2/\text{P(St-alt-MAN)}/\text{Ni-NTA}$, the fluorescence intensity of the His-tagged GFP solutions was

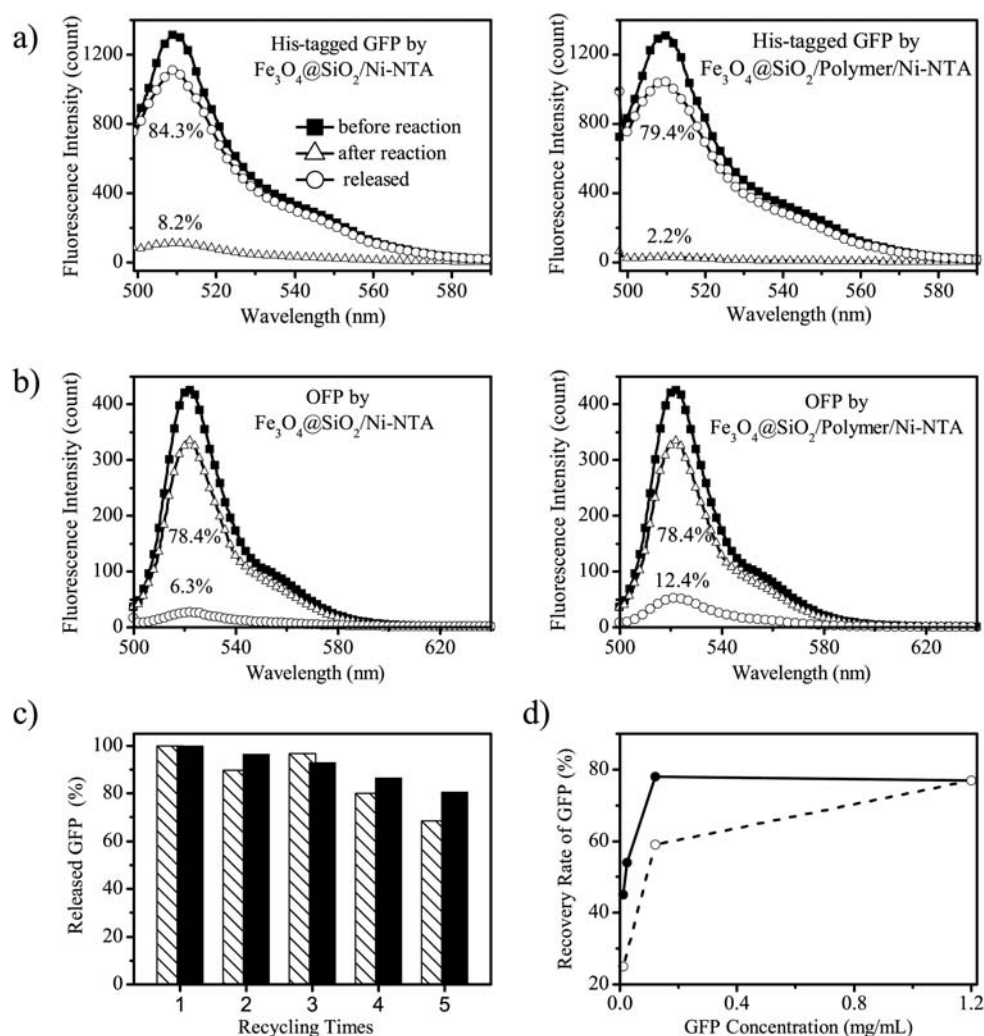


Fig. 4 Fluorescence spectra showing the change of emission intensity of the solutions of a) His-tagged GFP and b) non-tagged OFP before and after treated with Fe₃O₄@SiO₂/Ni-NTA (left) and Fe₃O₄@SiO₂/P(St-alt-MAA)/Ni-NTA (right). The curves with filled square symbols represent the fluorescence spectrum of the GFP/OFP solution before treating with nanoparticles. The curves with open triangle symbols are the spectra of the solution after treating with nanoparticles. The curves with open circle symbols represent the spectra of the solution after protein releasing from the nanoparticles. All solutions examined were in the same volume. The percentages of the fluorescence intensities shown are related to the initial fluorescence intensity of GFP/OFP. c) Recycling of Fe₃O₄@SiO₂/Ni-NTA (sparse bar) and Fe₃O₄@SiO₂/P(St-alt-MAA)/Ni-NTA (black bar) in the separation of GFP. d) The recovery rate of different-concentration His-tagged GFP by Fe₃O₄@SiO₂/P(St-alt-MAA)/Ni-NTA (solid line) and Fe₃O₄@SiO₂/Ni-NTA (dash line).

reduced to 8.2% and 2.2%, respectively, indicating the significant binding of GFP on both types of NTA-modified magnetic spheres. After washing with an imidazole solution for 10 min, 84.3% and 79.4% related to the original GFP was released from the Fe₃O₄@SiO₂/Ni-NTA and Fe₃O₄@SiO₂/P(St-alt-MAA)/Ni-NTA, respectively.

In a control experiment, orange fluorescent protein (OFP) without His-tag was used. When the OFP solution was treated with the same amount of Fe₃O₄@SiO₂/Ni-NTA or Fe₃O₄@SiO₂/P(St-alt-MAA)/Ni-NTA spheres, 22% decrease in the fluorescence intensity was observed for both spheres (Fig. 4b). After the magnetic spheres were washed with an imidazole solution, only 6.3% and 12.4% related to the original OFP were released from the magnetic spheres. The low adsorption and desorption capacities of OFP on the NTA-modified magnetic spheres can be attributed to the unspecified binding of OFP on the magnetic spheres.

The recyclability of the magnetic spheres in His-tagged protein separation was also investigated. After each separation, the magnetic spheres were rinsed with EDTA solution to release Ni²⁺ and clean the surface of the particles, then incubated with Ni(CH₃COO)₂ solution to introduce fresh Ni-NTA sites for the next separation. Recycling experiments were carried out for five times. The recyclability of both Fe₃O₄@SiO₂/Ni-NTA or Fe₃O₄@SiO₂/P(St-alt-MAA)/Ni-NTA spheres was evaluated by comparing the amount of separated GFP each time with the amount of GFP isolated in the first cycle. After five separation cycles, the separation capacity of the His-tagged protein was maintained at 68% for Fe₃O₄@SiO₂/Ni-NTA and 81% for Fe₃O₄@SiO₂/P(St-alt-MAA)/Ni-NTA, respectively (Fig. 4c). The better recycling stability of Fe₃O₄@SiO₂/P(St-alt-MAA)/Ni-NTA is attributed to abundant NTA sites on the magnetic polymer spheres.

Having more Ni-NTA sites on their surface, $\text{Fe}_3\text{O}_4@\text{SiO}_2/\text{P}(\text{St-alt-MAA})/\text{Ni-NTA}$ spheres were also expected to bind more His-tagged proteins than $\text{Fe}_3\text{O}_4@\text{SiO}_2/\text{Ni-NTA}$. To evaluate such an expectation, 6.0 μg His-tagged GFP was mixed with different amount of $\text{Fe}_3\text{O}_4@\text{SiO}_2/\text{Ni-NTA}$ or $\text{Fe}_3\text{O}_4@\text{SiO}_2/\text{P}(\text{St-alt-MAA})/\text{Ni-NTA}$ spheres (See Experimental Section for details). Based on fluorescence measurements, 48 μg of $\text{Fe}_3\text{O}_4@\text{SiO}_2/\text{Ni-NTA}$ -Ni(II) were requested to achieve $\sim 99\%$ adsorption of the proteins. Only 12 μg of $\text{Fe}_3\text{O}_4@\text{SiO}_2/\text{P}(\text{St-alt-MAA})/\text{Ni-NTA}$ spheres was able to complete the adsorption of the same amount of His-tagged GFP. These results indicated that $\text{Fe}_3\text{O}_4@\text{SiO}_2/\text{P}(\text{St-alt-MAA})/\text{Ni-NTA}$ spheres have a significantly higher adsorption capacity for His-tagged proteins than $\text{Fe}_3\text{O}_4@\text{SiO}_2/\text{Ni-NTA}$. More importantly, the more abundant binding sites in $\text{Fe}_3\text{O}_4@\text{SiO}_2/\text{P}(\text{St-alt-MAA})/\text{Ni-NTA}$ resulted in higher recovery of His-tagged protein from their low-concentration solutions (Fig. 4d). From a protein solution containing 1.2 $\mu\text{gGFP}/\mu\text{L}$, both $\text{Fe}_3\text{O}_4@\text{SiO}_2/\text{Ni-NTA}$ and $\text{Fe}_3\text{O}_4@\text{SiO}_2/\text{P}(\text{St-alt-MAA})/\text{Ni-NTA}$ recovered a similar amount of proteins, 76% and 77%, respectively. However, when the protein concentration was lowered to 0.12 and 0.012 $\mu\text{g}/\mu\text{L}$, the recovery rate by $\text{Fe}_3\text{O}_4@\text{SiO}_2/\text{Ni-NTA}$ was significantly decreased to 59% and 26%, respectively. In comparison, the protein recovery by

$\text{Fe}_3\text{O}_4@\text{SiO}_2/\text{P}(\text{St-alt-MAA})/\text{Ni-NTA}$ was 78%, 54% and 45% for the solutions with the concentrations of 0.12, 0.024, and 0.012 $\mu\text{g}/\mu\text{L}$, respectively. This observation can be reasonably explained by the more binding sites in polymer spheres, consistent with many reported multivalency phenomena in proteins binding.^{28,29}

To further examine the practical applications of the magnetic spheres for purification of His-tagged proteins, isopropyl beta-D-thiogalacto-pyranoside (IPTG) was used to induce *E. coli* to express His-tagged proteins. The functional spheres were then incubated with *E. coli* lysate, separated by a magnet, and washed with an imidazole solution to release His-tagged proteins. The purified His-tagged proteins were analyzed by SDS-PAGE. As illustrated in Fig. 5, the His-tagged proteins were nicely separated from the lysate by both $\text{Fe}_3\text{O}_4@\text{SiO}_2/\text{P}(\text{St-alt-MAA})/\text{Ni-NTA}$ spheres and $\text{Fe}_3\text{O}_4@\text{SiO}_2/\text{Ni-NTA}$ spheres. While 500 mM imidazole was required to release most His-tagged GFP bound on both $\text{Fe}_3\text{O}_4@\text{SiO}_2/\text{P}(\text{St-alt-MAA})/\text{Ni-NTA}$ and $\text{Fe}_3\text{O}_4@\text{SiO}_2/\text{Ni-NTA}$ spheres, 100 mM imidazole was enough to release most His-tagged human p16 from the magnetic spheres. The analysis showed that the magnetic spheres reported here hold promises for facile separation of His-tagged protein from cells lysates.

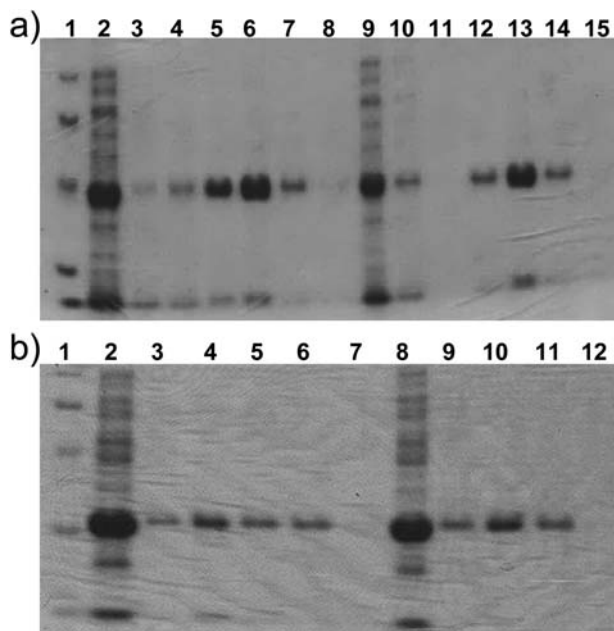


Fig. 5 a) SDS-PAGE analysis of proteins separated from crude *E. coli* lysate containing His-tagged GFP (Lane 2 and 9) by treated with $\text{Fe}_3\text{O}_4@\text{SiO}_2/\text{P}(\text{St-alt-MAA})/\text{Ni-NTA}$ (Lane 3–8) and $\text{Fe}_3\text{O}_4@\text{SiO}_2/\text{Ni-NTA}$ (Lane 10–15). Lane 1 is a molecular weight marker. Imidazole concentrations used in the protein release: 0.01M for Lane 3 and 10, 0.10 mM for Lane 4 and 11, 0.25 mM for Lane 5 and 12, 0.50 mM for Lane 6 and 13, 1.00 M for Lane 7 and 14, and 1.5M for Lane 8 and 15. b) SDS-PAGE analysis of proteins separated from crude *E. coli* lysate containing His-tagged human p16 (Lane 2 and 8) by treated with $\text{Fe}_3\text{O}_4@\text{SiO}_2/\text{P}(\text{St-alt-MAA})/\text{Ni-NTA}$ (Lane 3–7) and $\text{Fe}_3\text{O}_4@\text{SiO}_2/\text{Ni-NTA}$ (Lane 9–12). Lane 1 is a molecular weight marker. The concentrations of imidazole used in the protein release: 0.01M for Lane 3 and 9, 0.10 mM for Lane 4 and 10, 0.25 mM for Lane 5 and 11, 0.50 mM for Lane 6 and 12, and 1.00 M for Lane 7.

Conclusions

In summary, we have successfully synthesized superparamagnetic $\text{Fe}_3\text{O}_4@\text{SiO}_2/\text{P}(\text{St-alt-MAA})$ core-shell microspheres. Having poly(styrene-alt-maleic anhydride) as the shell, a larger number of Ni-NTA affinity sites were incorporated onto the surface of the magnetic spheres. Compared to the direct coupling of Ni-NTA groups on $\text{Fe}_3\text{O}_4@\text{SiO}_2$, the polymer mediated Ni-NTA modification endows the magnetic microspheres with significantly increased adsorption capacity of His-tagged proteins. The improved recovery of His-tagged protein from low-concentration solutions makes the as-prepared magnetic core-shell polymer microspheres promising for practical applications.

Acknowledgements

We thank NSFC (20925103, 20871100, 20721001), the Fok Ying Tung Education Foundation (121011), the 973 projects (2009CB930703) from MSTC, NSF of Fujian Province for Distinguished Young Investigator Grant (2009J06005) and the Key Scientific Project of Fujian Province (2009HZ0002-1).

Notes and references

- 1 E. Hochuli, H. Dobeli and A. Schacher, *J. Chromatogr., A*, 1987, **411**, 177.
- 2 Pedro Tartaj, M. d. P.M., Sabino Veintemillas-Verdaguer, Teresita González-Carreño and Carlos J. Serna, *J. Phys. D: Appl. Phys.*, 2003, **36**, R128.
- 3 J. Xie, K. Chen, H. Y. Lee, C. Xu, A. R. Hsu, S. Peng, X. Chen and S. Sun, *J. Am. Chem. Soc.*, 2008, **130**, 7542.
- 4 C. Corot, P. Robert, J. M. Idee and M. Port, *Adv. Drug Delivery Rev.*, 2006, **58**, 1471.
- 5 I. J. De Vries, W. J. Lesterhuis, J. O. Barentsz, P. Verdijk, J. H. van Krieken, O. C. Boerman, W. J. Oyen, J. J. Bonenkamp, J. B. Boezeman, G. J. Adema, J. W. Bulte, T. W. Scheenen,

- C. J. Punt, A. Heerschap and C. G. Figdor, *Nat. Biotechnol.*, 2005, **23**, 1407.
- 6 N. Kohler, C. Sun, A. Fichtenholtz, J. Gunn, C. Fang and M. Zhang, *Small*, 2006, **2**, 785.
- 7 C. Alexiou, R. J. Schmid, R. Jurgons, M. Kremer, G. Wanner, C. Bergemann, E. Huenges, T. Nawroth, W. Arnold and F. G. Parak, *Eur. Biophys. J.*, 2006, **35**, 446.
- 8 S. H. Kim, D. B. Asay and M. T. Dugger, *Nano Today*, 2007, **2**, 22.
- 9 U. Schillinger, T. Brill, C. Rudolph, S. Huth, S. r. Gersting, F. Krötz, J. Hirschberger, C. Bergemann and C. J. Plank, *J. Magn. Magn. Mater.*, 2005, **293**, 501.
- 10 A. Jordan, P. Wust, H. Fahling, W. John, A. Hinz and R. Felix, *Int. J. Hyperthermia*, 1993, **9**, 51.
- 11 Stéphane Mornet, S. b. V., Fabien Grasset and Etienne Duguet, *J. Mater. Chem.*, 2004, **14**, 2161.
- 12 F. Scherer, M. Anton, U. Schillinger, J. Henke, C. Bergemann, A. Kruger, B. Gansbacher and C. Plank, *Gene Ther.*, 2002, **9**, 102.
- 13 K. Kang, J. Choi, J. H. Nam, S. C. Lee, K. J. Kim, S. W. Lee and J. H. Chang, *J. Phys. Chem. B*, 2009, **113**, 536.
- 14 D. S. Wang, H. J. He, N. Rosenzweig and Z. Rosenzweig, *Nano Lett.*, 2004, **4**, 409.
- 15 J. Fan, J. Lu, R. Xu, R. Jiang and Y. Gao, *J. Colloid Interface Sci.*, 2003, **266**, 215.
- 16 S. Bucak, D. A. Jones, P. E. Laibinis and T. A. Hatton, *Biotechnol. Prog.*, 2003, **19**, 477.
- 17 C. Xu, K. Xu, H. Gu, X. Zhong, Z. Guo, R. Zheng, X. Zhang and B. Xu, *J. Am. Chem. Soc.*, 2004, **126**, 3392.
- 18 C. Xu, K. Xu, H. Gu, R. Zheng, H. Liu, X. Zhang, Z. Guo and B. Xu, *J. Am. Chem. Soc.*, 2004, **126**, 9938.
- 19 J. S. Kim, C. A. Valencia, R. Liu and W. Lin, *Bioconjugate Chem.*, 2007, **18**, 333.
- 20 H. Zhu, M. Bilgin, R. Bangham, D. Hall, A. Casamayor, P. Bertone, N. Lan, R. Jansen, S. Bidlingmaier, T. Houfek, T. Mitchell, P. Miller, R. A. Dean, M. Gerstein and M. Snyder, *Science*, 2001, **293**, 2101.
- 21 I. S. Lee, N. Lee, J. Park, B. H. Kim, Y. W. Yi, T. Kim, T. K. Kim, I. H. Lee, S. R. Paik and T. Hyeon, *J. Am. Chem. Soc.*, 2006, **128**, 10658.
- 22 K. S. Lee and I. S. Lee, *Chem. Commun.*, 2008, 709.
- 23 K. Jaeyun, P. Yuanzhe, L. Nohyun, P. Yong Il, L. In-Hwan, L. Jung-Ho, R. P. Seung and H. Taeghwan, *Adv. Mater.*, 2010, **22**, 57.
- 24 H. Deng, X. Li, Q. Peng, X. Wang, J. Chen and Y. Li, *Angew. Chem., Int. Ed.*, 2005, **44**, 2782.
- 25 R. Satishkumar and A. Vertegel, *Biotechnol. Bioeng.*, 2008, **100**, 403.
- 26 C. Hemei, D. Chunhui and Z. Xiangmin, *Angew. Chem. Int. Ed.*, 2010, **49**, 607.
- 27 G.-M. Qiu, B.-K. Zhu, Y.-Y. Xu and K. E. Geckeler, *Macromolecules*, 2006, **39**, 3231.
- 28 S. Lata, M. Gavutis, R. Tampe and J. Piehler, *J. Am. Chem. Soc.*, 2006, **128**, 2365.
- 29 S. Lata, A. Reichel, R. Brock, R. Tampe and J. Piehler, *J. Am. Chem. Soc.*, 2005, **127**, 10205.